Numerical simulation of the unsteady flowfield in complete propulsion systems

Michele Ferlauto[a] and Roberto Marsilio[*]

*Department of Mechanical and Aerospace Engineering, Politecnico di Torino,
Cors Duca degli Abruzzi, 24, 10129, Torino, Italy*

Abstract.   A non-linear numerical simulation technique for predicting the unsteady performances of an air-breathing engine is developed. The study focuses on the simulation of integrated propulsion systems, where a closer coupling is needed between the airframe and the engine dynamics. In fact, the solution of the fully unsteady flow governing equations, rather than a lumped volume gas dynamics discretization, is essential for modeling the coupling between aero-servoelastic modes and engine dynamics in highly integrated propulsion systems. This consideration holds for any propulsion system when a full separation between the fluid dynamic time-scale and engine transient cannot be appreciated, as in the case of flow instabilities (e.g., rotating stall, surge, inlet unstart), or in case of sudden external perturbations (e.g., gas ingestion). Simulations of the coupling between external and internal flow are performed. The flow around the nacelle and inside the engine ducts (i.e., air intakes, nozzles) is solved by CFD computations, whereas the flow evolution through compressor and turbine bladings is simulated by actuator disks. Shaft work balance and rotor dynamics are deduced from the estimated torque on each turbine/compressor blade row.

1. Introduction

In high-performance propulsion systems, the actual working conditions are very close to critical modes as compressor stall or inlet unstart. Future vehicles proposed for supersonic commercial flights are also characterized by a long, slim body with pronounce aero-servoelastic modes (Kopasakis *et al*. 2010). In general, the modern engine concepts are moving toward highly integrated, multi-architecture propulsion systems which include more than one engine type in the same system (e.g., over-under TBCC engines, McDaniel 2012), or have a variable thermodynamic cycle (Fernandez-Villace and Paniagua 2013, Zheng *et al*. 2017). In many cases, engine-airframe integration effects performances and the fully unsteady treatment of the fluid dynamics inside and outside the engine must be taken into account for a reliable simulation of the propulsion system dynamics and for control purpose (see Benek *et al*. 1998, Litt *et al*. 2015).

Mathematical modelling and system simulation are generally used to resolve propulsion system

---

[*]Corresponding author, Associate Professor, E-mail: roberto.marsilio@polito.it
[a]Assistant Professor, E-mail: michele.ferlauto@polito.it

design problems throughout a development program. In this way, expensive wind-tunnel and flight-test programs may be minimized. While accurate CFD prediction of the flowfield of a single engine component is now feasible, a long-length unsteady simulation of the complete engine configuration remains too computationally expensive, (Litt *et al.* 2015, Chang *et al.* 2014, Lytle 1999). In fact, long-length unsteady simulations required to analyze the engine transient must deal with very different time-scales ranging from combustion process to flow unsteadiness, to rotor dynamics. Therefore, simplifications are put forward in order to make the problem affordable. Since the combustion processes and the real gas effects are approximated by empirical constitutive laws, one has to consider at least two time scales related to low-frequency and high-frequency unsteady phenomena, respectively. The low-frequency transients are related to the rotors dynamics and their relatively large inertia. The range in time of these phenomena is of the order of magnitude of some seconds (e.g., the time need to reach the maximum thrust from idle). The high-frequency transients are strictly related to fluid dynamic phenomena such as the pressure wave propagation through the engine: the range in time amounts to some hundredth or tenths of seconds. Temperature dynamics and the heat transfer process that effects the system efficiency have a secondary role, (Kopasakis *et al.* 2010).

For evaluating the unsteady performances for normal operations of many propulsion systems, the low frequency transients are of relevance. In this case, the use of Lumped Volume Models (LVM) of the engine components has shown to be appropriate, (Parker and Guo 2003, Federick *et al.* 2007, Wang 2011). These methods are based on the lumped volume representation of gas dynamics, (Seldner *et al.* 2007, Sellers *et al.* 1974), and on the assumption that the performances of each engine component are given by a steady-state map. This approximation holds in virtue of the large separation between the time scales of the fluid dynamics and the rotor dynamics. Moreover, when the typical dynamic characteristics of the actuation system are considered, the overall response of the system becomes even slower. A second order correction as regard the gas dynamics is introduced by the volume dynamics, which is based on a rough numerical approximation of the flow governing equations via mass and energy storage effects in control volumes associated with each component of the engine, Sellers *et al.* (1974). This formulation is applied by both analytical and numerical techniques, in case of frequency of about 10 Hz. When the strongly nonlinear unsteadiness that characterize fluid dynamic phenomena take place, these approximations are not valid anymore. The unsteadiness may arise from an external source, as in the case of a sudden change of inlet conditions. More frequently, the unsteadiness is due to the aerodynamic coupling between the engine components or to flow instabilities, (Ferlauto and Rosa Taddei 2015). It has been demonstrated that the interaction cannot be represented by ad hoc boundary conditions, Sajben (2004). The resolution of the flow at this finer time-scale becomes essential to derive the correct dynamics. For high-frequency transients, the interest is focused to predict the pressure waves propagation by looking inside the single engine's component. The engine model must be reliable in describing the actual unsteady process occurring in the system component (compressor, turbine, etc.). We are therefore led to a more complex modelling framework for the long length scale unsteady simulation of turbomachinery flows, Hynes and Denton (2003), which also allows to investigate the evolution of perturbations inside the engine, off-design and critical conditions, as well as active control strategies, (Litt *et al.* 2015, Culley *et al.* 2009).

In the present work, flows inside and around an aero engine model are simulated. Aim of the research was to extend the approach proposed in Ferlauto *et al.* (2002) to a general configuration of a modern engine. The flow inside components as air intake and nozzles are evaluated by
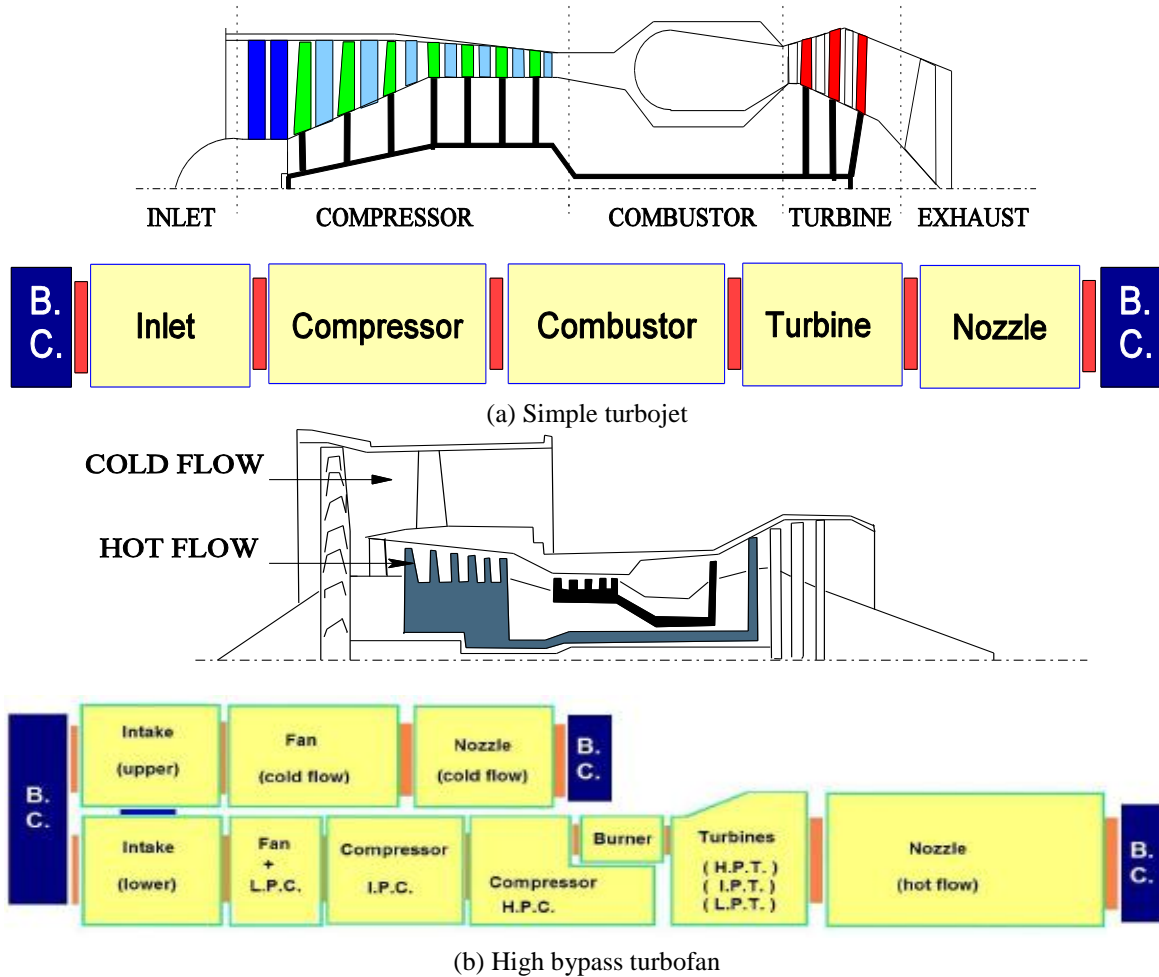
(a) Simple turbojet

(b) High bypass turbofan

Fig. 1 Schematic sketch of turbo-engines and modules

standard CFD techniques, while other components are simulated as 'black-boxes' or by low order models or actuator disks, Horlock (1978). The response of the models adopted is of the order of the fluid dynamic time scale, so that high frequency unsteadiness are correctly treated. For instance, each turbine/compressor blade row is simulated in a fashion similar to the model proposed in Ferlauto and Rosa Taddei (2015), Schmidtmann and Anders (2001) and Leonard and Adam (2008) to investigate rotating stall and to simulate a complete engine configuration, Marsilio (2005), Feraluto and Marsilio (2009). The flow is assumed axisymmetric and governed by the Euler equations, while the effects related to viscosity and secondary flows are considered by semi-empirical formulation deduced from experimental data and included in the low order models. The outline of the paper is as follows: after a short description of the mathematical model for the flow and the engine components, the capability of the numerical tool are investigated both in their one-dimensional and quasi-3D formulation.

2. The numerical approach

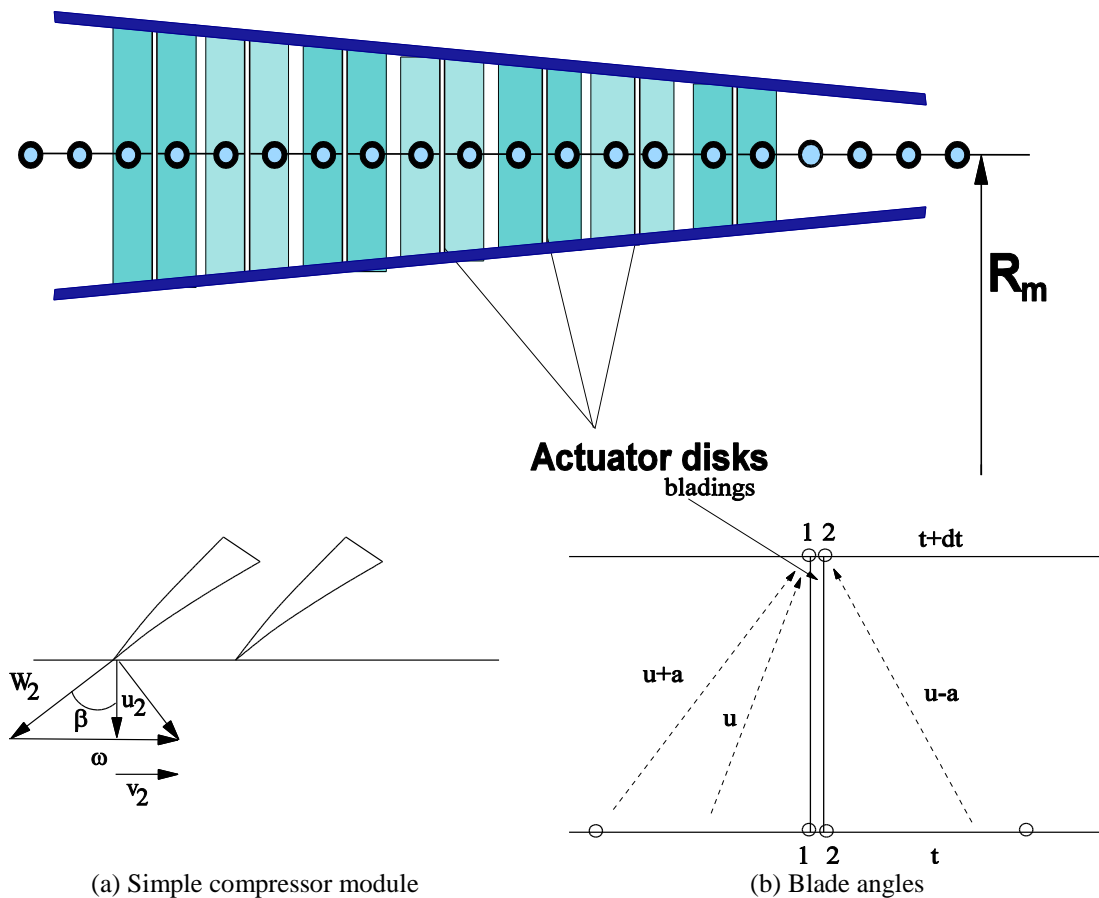(a) Simple compressor module   (b) Blade angles

Fig. 2 Actuator disks configuration and blade angles

The flowfield around the engine is simulated by a standard CFD technique. Depending on the relevance of the engine airframe interaction, the full resolution of the flowfield is extended to the engine nozzles and inlet. The engine core, instead, is represented by a lower-order CFD model. The reason for this simplification is partly due to the computational cost of a fully engine simulation, and partly related to the amount of detailed information otherwise required. Let us note that the method proposed here is based on the fully unsteady quasi-one-dimensional mean-radius description of the engine system. Therefore, if compared to a lumped volume model, i.e., an essentially 0-D model, different type and quality of information is needed to define the engine and its operating conditions. In the LVM approach just the macro-components defining the engine, their interconnections and manometric maps need to be defined. In the method, here proposed the details goes from the flow-path to the single blade row geometry.

In the original approach, Ferlauto and Marsilio (2009), a simple turbojet was represented as a single block: a quasi-one-dimensional distribution with cross-sectional areas assigned. Within this single computational domain were inserted turbomachinery components modelled as actuator disks. In this new approach to represent more complex engine architecture the following elements are introduced:

• modules;

• components models (actuator disk, black boxes);
• external environment models (flight conditions and boundary conditions);
• connection modules and routing modules.

The module is the basic container, within which are defined one or more components models. Every module is represented by a quasi-1D computational domain, incorporating logical connections and containing one or more elements (actuator disks or black-boxes). A complex engine configuration can be defined by a series of modules interconnected. For example, a meridian section of a simple turbojet with a possible division into modules and its block-diagram are visible in Fig. 1(a). In this case, five modules connected in series have been used, (air-intake, compressor, combustor, turbine and nozzle). Fig. 1(b) shows a more complex configuration for a high bypass modern turbofan.

2.1 Numerical method

As reported previously, the philosophy of choice for the development of numerical code is based on a modular approach (engine module). The whole engine can be broken down into its constituent modules. The engine represented in Fig. 1, for instance, can be seen as the set of five separate modules (compressor, combustion chamber, turbine and the exhaust system) suitably interconnected. Each engine module appears to be an independent unit capable of exchanging information with other modules and / or with the external environment by means of appropriate boundary conditions.

More complex configurations need to deal with more engine modules. Fig. 1(b) is showing a modern high-bypass turbofan described using ten component modules. The modular architecture allows to separate the engine from the numerical method making it easier to run simulations. The fluid dynamic field in each module will be determined numerically using a CFD method. Each module will be in conjunction with the adjacent through appropriate boundary conditions, fluid dynamics and/or mechanical ones. In this way, it will be possible to simulate the operation of the engine in various operating conditions.

In each engine module, its domain of integration is represented by the distribution of the axial cross section ("Flow-Path"), inlet and outlet boundary, and rotor and stator bladings, if present, inside the module (rotors and/or stators for compressor and turbine modules, Fig. 2). The flowfield inside the module is then solved by a CFD calculation.

The motion of the gas through a compressor, for instance, represents one of the most complicated example of fluid dynamics flowfield. Therefore, one must make some drastic simplification to get the models suitable to be treated by some algorithm. In the model presented in this paper the effect related to viscosity and secondary flows are neglected; however, any of these effects may be easily implemented by taking information from experimental data. The flow is assumed axisymmetric with negligible radial gradients. The problem is assumed to be quasi-1D in which the variation of the flow properties occurs only along the machine axis. The blading (which is a finite axial length) is reduced to a surface of discontinuity, normal to the machine axis. The deflection of the flow is supposed to take place through this discontinuity, according to the well-known "actuator disc theory", Horlock (1978). In other words, the two basic phenomena of the gas motion relative to the blading is splitted in two parts: the deflection, which is related to the aerodynamic load on the blades, occurs at the discontinuity; the pressure wave propagation, which is given by the unsteadiness, takes place along the machine, in the same axial length of the original blading. The modeling of the combustion chamber is even a tougher problem. Beside the

additional uncertainties in describing chemical process of the combustion in unsteady flow, the fluid dynamics is here very complicated. So far, in this work, the fuel heat input has been concentrate at a surface of discontinuity, and leave the actual length of the chamber for the pressure wave propagation. Other elements (exhaust nozzle and inlet) do not need any modelling, but the usual quasi-1D hypothesis. Real gas effects are considered using the NASA chemical database.

The numerical method will replace each blading, of both compressor and turbine, by actuator discs. The combustion chamber is imagined as a surface of continuity where the heat inputs are given, according to the prescribed fuel injection. At this point the engine is divided in many regions each of these, has left and right boundaries (surface of discontinuity). The flow is continuous through these regions. The unsteady quasi-1D flow equations are written in each region and integrated in time using a quasi-1D, CFD code developed in Marsilio (2005).

The governing equation of the flow are the time-dependent Euler equations written in their integral form as

$$\frac{\partial}{\partial t}\int_v \overrightarrow{W}\, dv + \int_S \vec{F}_I \, \cdot \, \vec{n}\, dS = 0 \tag{1}$$

where v represents an arbitrary volume enclosed in a surface S, $\overrightarrow{W}$ is the hyper-vector of conservative variables and tensor $\vec{F}_I$ contains the inviscid fluxes:

$$\overrightarrow{W} = \{\rho, \rho\vec{q}, E\}^T \tag{2}$$

$$\vec{F}_I = \{\rho, p\,\bar{I} + \rho\vec{q}\,\times\,\vec{q}, (e+p)\vec{q}\} \tag{3}$$

Quantities ρ, p and $\vec{q} = \{u, v\}$ are the local density, pressure and velocity, respectively. E is the total energy for unit volume

$$E = \rho\left(e + \frac{q^2}{2}\right) \tag{4}$$

where e is the internal energy for unit mass and $\bar{I}$ is the identity matrix. The perfect gas relationship completes the set of equations. System (1) can be reduced to non-dimensional form with the help of the following reference values: L_{ref} for length, ρ_{ref} for density, T_{ref} for temperature, $\sqrt{RT_{ref}}$ for velocity and RT_{ref} for energy.

System (1) is discretized according to a finite volume technique where the convective part of the equations is treated by a Flux Difference Splitting method with an approximate Riemann Problem Solver. The flowfield is decomposed into regions fully resolved by CFD (e.g., the external flow, nozzles, inlet) and very small regions replaced by low order models (e.g., the bladed disks). This reduction allows for an effective simulation of the engine transients with acceptable CPU time. Moreover, the low order modelling also greatly simplifies a further introduction of the engine control systems. The internal and the external computations will be coupled by appropriate boundary conditions.

2.2 External flow and boundary conditions

External flow and other elements like exhaust nozzle and inlet do not need any modelling, and they will be solved by the axisymmetric CFD computations. The governing equations of the flow

are the same used to compute the internal flow (1). Second order accuracy is achieved following the guidelines of the Essentially Non-Oscillatory schemes (ENO), with linear reconstruction of the solution inside each cell and at each step of integration, (Harten *et al.* 1987).

The computation at the boundaries is carried out by solving a half Riemann problem (Ferlauto *et al.* 2002). Briefly, in the same spirit of the Flux-Difference Splitting method used at the internal cells interfaces, (Ferlauto and Rosa Taddei 2015), the boundary fluxes are evaluated from a combination of boundary conditions and wave-system signals reaching the border from inside.

The number of conditions to be given at the boundary is therefore prescribed by the number of characteristic lines irradiated from the border toward the inner field, while their quality is dictated by the physics of the problem to be solved. The computational domain is bounded by artificial (e.g., far field or permeable boundaries as inlet and outlet) and physical contours (e.g. impermeable walls). At subsonic inlets three boundary conditions are needed. We impose total pressure, total temperature and the flow angle. In the supersonic case, all the flow variables are prescribed. Conversely at the outlet, one boundary condition is needed for subsonic flows, while none is needed for supersonic flows. Usually the static pressure is prescribed at subsonic outlets. At the walls one boundary condition is needed. At solid walls, the impermeability imposes the vanishing of the normal velocity component.

2.3 Compressor and Turbine bladings

Each blading (which presents a finite axial length) is reduced to a surface of discontinuity normal to the machine longitudinal axis. The deflection of the flow is supposed to take place through this discontinuity, according the "actuator disk theory", (Horlock 1978, Chernyshenko and Privalov 2004). The basic phenomena of the gas motion relative to the blading are splitted in two parts: the deflection, which is related to the aerodynamic load on the blades, occurs at the discontinuity; the pressure wave propagation, which is given by the unsteadiness, takes place along the machine, in the same axial length of the original blading. The technique used to solve the actuator disk problem is very similar to the "shock-fitting" method, Marsilio (2005). Briefly, the quasi-steady relationships obtained express the continuity, momentum and energy balance with geometrical constrains. These conditions will be matched with the compatibility equations (along the characteristic lines) in the regions which bound the discontinuity, to provide the flow properties on the two sides of the discontinuity. The quasi-steady relationships at the disc, which are replacing the blading, are

$$\begin{cases} \dfrac{u_1 p_1}{h_1} = \dfrac{u_2 p_2}{h_2} \\ h_2 + \dfrac{1}{2}(u_2^2 + v_2^2) = h_1 + \dfrac{1}{2}(u_1^2 + v_1^2) + \\ \qquad \sigma\omega(v_2 - v_1) \\ \qquad S_2 = S_1 \\ v2 = \sigma\omega - u_2 \tan\beta \end{cases} \tag{5}$$

$$\frac{u_1 p_1}{T_1} = f\left(p_{1,rel}^0, T_{1,rel}^0, \beta\right) \tag{6}$$

where $p_{1,rel}^0$ and $T_{1,rel}^0$ are the total values of pressure and temperature of the flow relative to the blading. Using Eq. (6) the point 1 is computed by considering the compatibility equation onto the
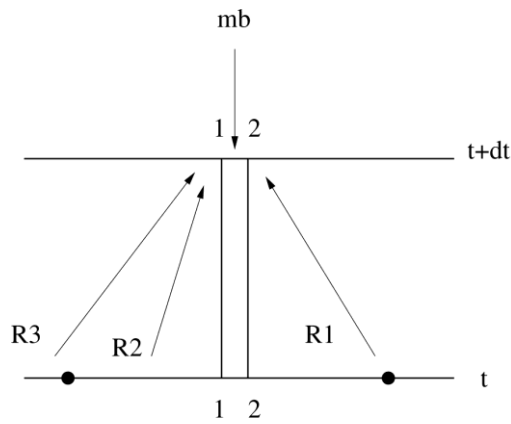
Fig. 3 Actuator disk for combustor

upstream part of the disc. To compute the point 2 the continuity equation with the isentropic assumption will be used. The modulus of the relative velocity w_2 at the trailing edge will follows as

$$w_2^2 = \frac{2\gamma}{\gamma - 1}\left(T_{1,rel}^0 - T_2\right) \tag{7}$$

the direction of w_2 will be in general different from the one given by β. Finally, the downstream tangential velocity is computed as

$$v_2 = \sigma\omega - \sqrt{w_2^2 - u_2^2} \tag{8}$$
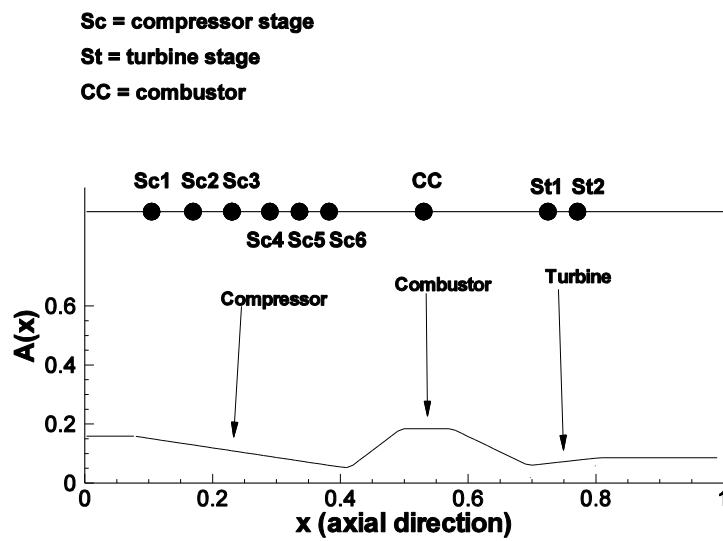
for subsonic axial flows.

Fig. 4 Internal turbojet schematization

2.4 Combustor and afterburner

The modelling of the combustion and afterburner chamber is a very complex problem. So far, at this level of code development the fuel combustion is treated by a disk actuator, and leave the actual length of the chamber for the pressure wave propagation. The combustion chamber is treated as surface of discontinuity where the heat inputs are given, according to the prescribed fuel injection.

The conditions to be imposed on the disk will be continuity, momentum and energy balance. Referring to Fig. 3 these relationships may be written as

$$
\begin{cases}
\dfrac{u_1 p_1}{h_1} + \dot{m}_b = \dfrac{u_2 p_2}{h_2} \\[2mm]
p_1 \left(1 + \dfrac{\gamma - 1}{\gamma} \dfrac{u_1^2}{h_1} \right) = p_2 \left(1 + \dfrac{\gamma - 1}{\gamma} \dfrac{u_2^2}{h_2} \right) \\[2mm]
v_2 = v_1 \\[2mm]
\dot{m}_a (h_2^0 - h_1^0) = \dot{m}_b \, H_i
\end{cases}
\tag{9}
$$

where h_1^0 and h_2^2 are the total enthalpy in region 1 and 2, respectively. The energy equation (last of Eq. (9)) takes into the account the heat release where $\dot{m}_a, \dot{m}_b$ and H_i represent the air mass flow, the fuel mass flow and the fuel heating values referred to $c_v T_{ref}$.

Alternatively, the integral model proposed in Ferlauto *et al.* (2002) can be adopted. In that case, a source term is appearing into the flow governing equations to consider the heat release during combustion.

2.5 Inlet, nozzle and other ducts

Inlets and nozzles may be modelled with three different levels of approximation. First, the flow inside the inlet and nozzle is solved together with the external flow by using the same solver, with
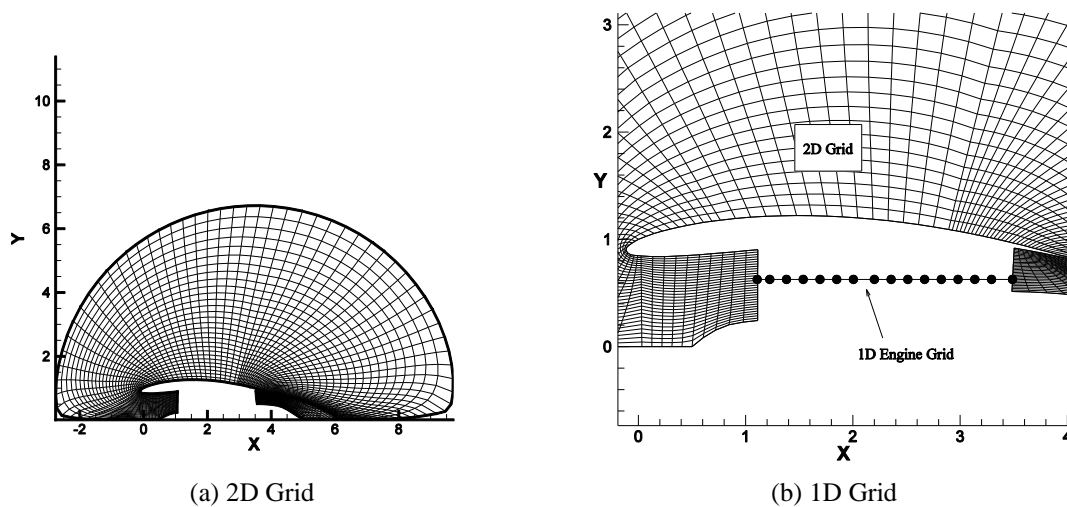

(a) 2D Grid   (b) 1D Grid

Fig. 5 Computational external and internal grids

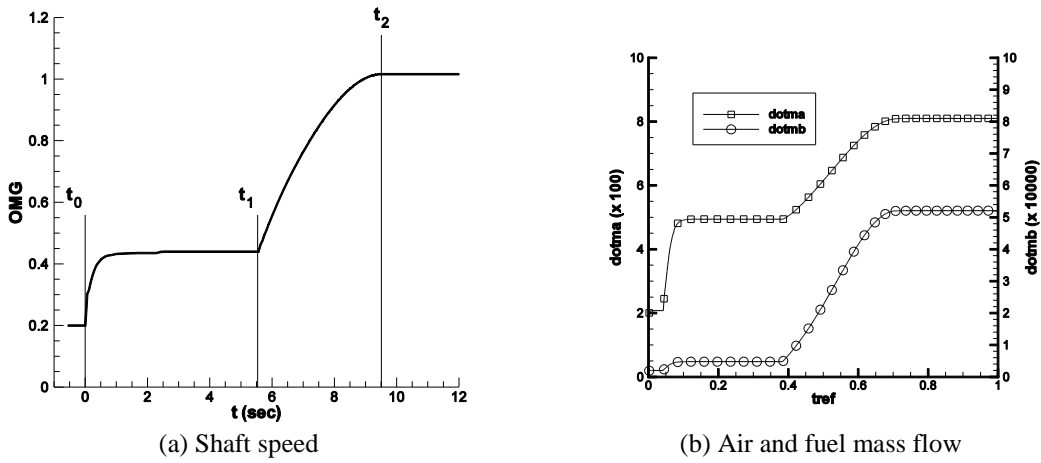(a) Shaft speed   (b) Air and fuel mass flow

Fig. 6 Engine transient simulations

the advantage of having good resolutions of the engine inlet and outlet regions. Second, a quasi-1D reduction of the flow problem is adopted. Many relevant details of the flow are lost, but the model still gives the variation of the flow properties along the duct. The third solution is the actuator disk approach, Horlock (1978). In this case only the variation between duct inlet and outlet is available.

Although this can be a very rough approximation for inlet or nozzle, the model is very useful to simulate valves or bleed ducts.

2.6 Rotor dynamics

The operating line of a turbojet engine is the locus of steady state performance match points between the compressor and turbine. A mismatch between these components produces an unbalanced torque, which must be integrated by a dynamic relation to change the rotational speed and seek for a steady state match. The relation governing the rotor dynamics can be written in term of the angular momentum.

$$\frac{d(J\omega)}{dt} = \Delta C \tag{10}$$

where ΔC is the torque excess and J is the inertia value of the rotor system, respectively, Eq. (10) is integrated in time together with the flow equations.

3. Engine simulation

With a view to validating the engine model, a simple one-spool turbojet scheme has been chosen. The engine core is formed by a six stages axial compressor driven by a two stages turbine with the following parameters: engine length equal to $L_{ref} = 1.45$ meters, external diameter of the 1st compressor equal to $d_c = 1.0$ meters, mean engine radius is equal to $r_{mean} = 0.275$ meters, nominal revolution speed is $n = 10500$ rpm with a nominal mass flow of $\dot{m} = 60$ kg/s.

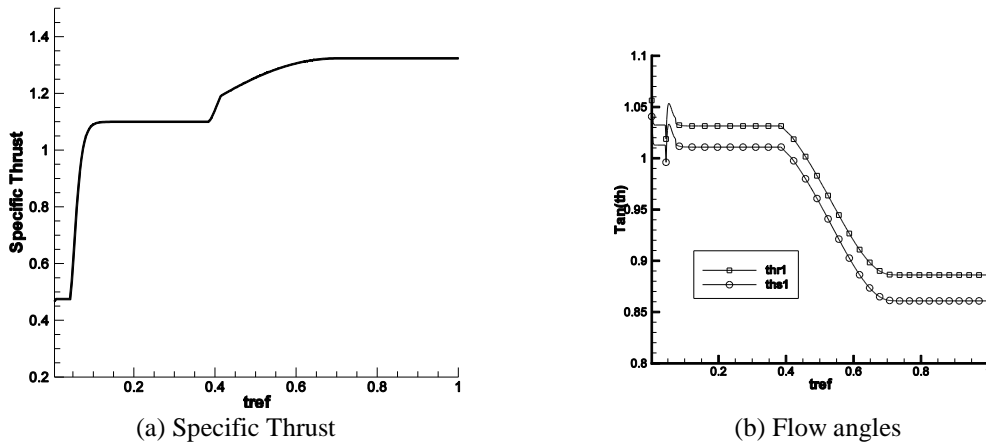(a) Specific Thrust   (b) Flow angles

Fig. 7 Engine transient simulations

The schematic distribution of the actuator discs and the relative cross area distribution along the engine axis is shown in Fig. 4. In Fig. 4, the compressor stages (rotor and stator) are labelled by Sc, the turbine stages (diffuser and rotor) are labelled by St and the combustion chamber is indicated by CC.

Fig. 5 shows the numerical grid for the external and the internal geometry used for the engine model simulation.

All computations have been carried out on a 100 grid points for the internal flow (engine 1-D)

and on a 100×30 points for the external, 2-D grid. The geometric angle β at the trailing edge has been chosen equal to 30 deg. for compressor blading and 63 deg. for turbine blading, respectively.

Two transients have been computed within the same simulation. The first deals with the starting of the engine, the second with the variation in time of the throttle. Before going further, few words need to be spent regards this preliminary stage of investigation. In real engines simulation, the starting operation takes a relatively long time, because of the limited torque available from the starting device and the very high inertia of the rotors.

It should be noted that, at these first stages of investigation, some of the model parameters may be not well assessed (e.g., the rotors inertia). For this reason, a very fast (even if unrealistic) starting engine procedure has been obtained and presented in Fig. 6. Regarding Fig. 6, times t_0, t_1 and t_2 separate different temporal phases:

- For $(t \leq t_0)$: the throttle is in idle and the engine is supposed to be driven by an Auxiliary Power Unit (APU);

- For $(t_0 < t \leq t_1)$: turbine is now driving the compressor, so that the rotor speed is depending by the instantaneous difference in torques on turbine and compressor, and on rotor inertia. The throttle is in idle and the engine is self-sustained, (the self-sustained speed is about 45% of the nominal design speed, $t > t_2$);

- For $(t > t_1)$: the throttle is increasing till a maximum value $(t = t_2)$ and the engine increase its rotational speed until the steady configuration is reached.

Fig. 6(a) shows the variation in time (sec) of the no dimensional rotational speed (Shaft Speed), ω, during the three different phases above described. t_{ref} represents the physical time scaled from 0 to 1

$$t_{ref} = \frac{t - t_{min}}{t_{max} - t_{min}}, (t_{min} = 0\ s, t_{max} = 12\ s \tag{10}$$

There are many information and output values which may be obtained from these computations; for example, the normalized air mass flows $\dot{m}_a$ and the fuel mass flow $\dot{m}_b$ are reported in Fig. 6(b) and the normalized specific thrust is shown in Fig. 7(a). Mass flows and specific thrust have been normalized with respect to $\dot{m}_{ref} = \rho_{ref} U_{ref} L_{ref}^2$, $U_{ref} = \sqrt{RT_{ref}}$, respectively. The time evolution of the inlet flow angle (in degree) on the first rotor (thr1) and on first stator (ths1) of the compressor is shown in Fig. 7(b).

Figs. 8(a), 8(b) show the total pressure ratio, P_0, the total temperature ratio, T_0, and the axial Mach number distribution along the machine axis reached at time $t > t_2$, in a full throttle condition and when the steady state configuration is reached. The corresponding unsteady external flow evolution (for $0 \leq t \leq t_2$) is reported in terms of Mach number contours in Fig. 9.

5. Conclusions

A numerical method based on CFD approach for predicting the performances given by gas turbine engines during transient has been developed. The full equations describing this phenomenology are integrated in time according to a finite volume procedure. The bladings and the combustor have been modeled by actuator disks. The time-dependent approach allows for the computation for high frequency transients inside the machine elements. The main feature of the present methodology are: the compressible effects are taken into account; the capability of investigating flow field with several kinds of distortion; the easy extension to 3D flow; the interaction between the engine and the external flow is inherently accounted for. Further improvements are needed to include real gas effects, more adequate loss models and parameter assessments, models of the engine control systems.
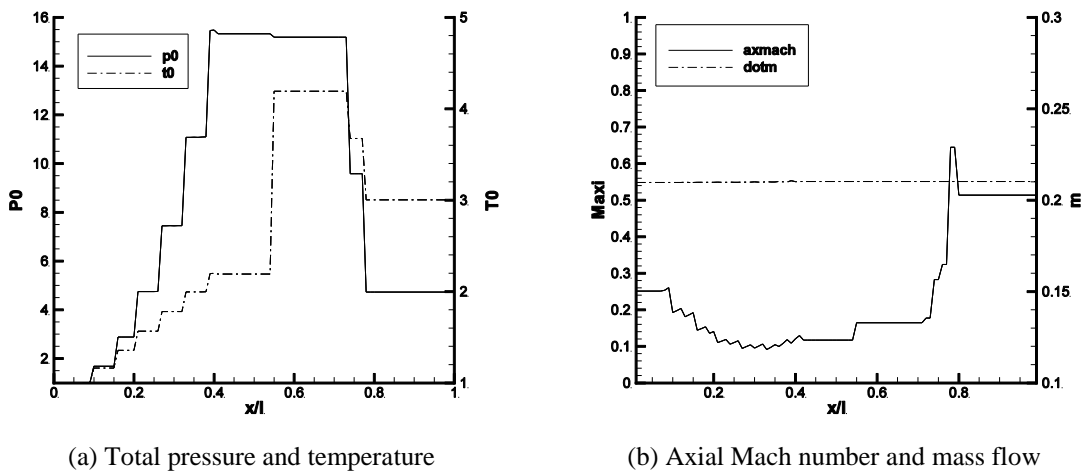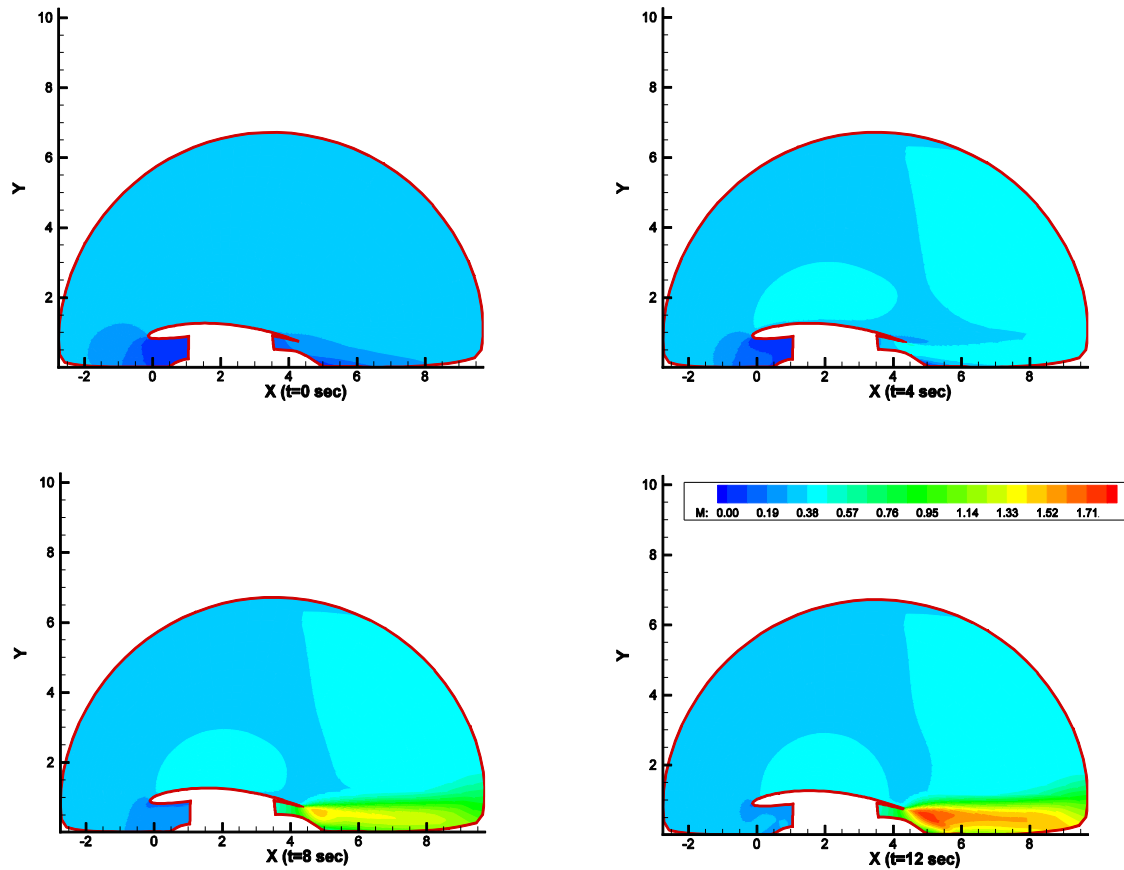

(a) Total pressure and temperature   (b) Axial Mach number and mass flow

Fig. 8 Steady state values

Fig. 9 Mach number contours of the external flow during engine transient

Acknowledgments

References

Benek, I.A., Kraft, E.M. and Lauer, R.F. (1998), "Validation issues for engine-airframe integration", *AIAA J.*, 36(5),759-764.

Chang, H., Zhao, W., Jin, D., Peng, Z. and Gui, X. (2014), "Numerical investigation of base-setting of stators stagger angles for a 15-stages axial flow compressor", *J. Therm. Sci.*, **23**(1), 36-44.

Chernyshenko, S.I. and Privalov, A.V. (2004), "Internal degree of freedom of an actuator disk model", *J. Propul. Power*, **20**(1), 155-163.

Culley, D., Garg, S., Hiller, S.J., Horn, W., Kumar, A., Mathews, H.K. and Schadow, K. (2009), *More*

Intelligent Gas Turbine Engines, RTO-TR-AVT-128.

Ferlauto, M., Larocca, F. and Zannetti, L. (2002), "Integrated design and analysis of intakes and nozzles in airbreathing engines", *J. Propul. Pow.*, **18**(1), 28-34.

Ferlauto, M. and Marsilio, R. (2009), "Numerical simulation of transient operations in aeroengines", *Proceedings of the 8th European Conference on Turbomachinery Fluid Dynamics and Thermodynamics (ETC8)*, Graz, Austria, March.

Ferlauto, M. and Rosa Taddei, S. (2015), "Reduced order modelling of full-span rotating stall for the flow control simulation of axial compressors", *Proceedings of the Institution of Mechanical Engineering Part A: Journal of Powez Energy*, **229**(4), 359-366.

Fernandez-Villace, V. and Paniagua, G. (2013), "Numerical model of a variable-combined-cycle engine for dual subsonic and supersonic cruise", *Energies*, **6**(2), 839-870.

Frederick, D.K., DeCastro, J.A. and Litt, J.S. (2007), *User's Guide for the Commercial Modular Aero-Propulsion System Simulation(C-MAPPS)*, NASA Report No. TM-2007-215026.

Harten, A., Engquist, B., Osher, S. and Chakravarthy, S.R. (1987), "Uniformly high order accurate essentially non-oscillatory schemes, III", *J. Comput. Phys.*, **71**(2), 232-303.

Horlock, J.H. (1978), *Actuator Disk Theory*, McGraw-Hill, U.S.A.

Kopasakis, J., Connolly, J.W., Paxson, D.E. and Ma, P. (2010), "Volume dynamics propulsion system modeling for supersonics vehicle research", *ASME J. Turbomach.*, **132**(4), 041003.

Leonard, O. and Adam, O. (2008), "A quasi-one- dimensional model for multistage turbomachinery", *J. Therm. Sci.*, **17**(1), 7-20.

Litt, J.S., Liu, Y., Sowers, T.S., Owen, K. and Guo, T.H. (2015), "Validation of an integrated airframe and turbofan engine simulation for evaluation of propulsion control modes", *Proceedings of the 53rd AIAA Aerospace Sciences Meeting*, *AIAA SciTech Forum*, Florida, U.S.A., January.

Lytle, J.K. (1999), "The numerical propulsion system simulation: A multidisciplinary design system for aerospace vehicles", *Proceedings of the 14th International Symposium on Air Breathing Engines*, Florence, Italy, September.

Marsilio, R. (2005), "A computational method for gas turbine engines", *Proceedings of the 53rd AIAA Aerospace Sciences Meeting*, *AIAA SciTech Forum*, Florida, U.S.A., January.

McDaniel, J. (2012), "An overview of the national center for hypersonic combined-cycle propulsion", *Proceedings of the NASA 2012 Fundamental Aeronautics Program Annual Meeting*, Cleveland, U.S.A., March.

Parker, K.L. and Guo, T.H. (2003), *Development of a Turbofan Engine Simulation in Graphical Simulation Environment*, NASA Report No TM-2003-213543.

Sajben, M. (2004), "Model for multistage compressors to predict unsteady inlet-compressor interactions", *J. Propul. Pow.*, **20**(3), 492-500.

Schmidtmann, O. and Anders, J.M. (2001), "Route to surge for a throttled compressor - a numerical study", *J. Fluids Struct.*, **15**(8), 1105-1121.

Seldner, K., Mihaloew, J.R. and Blaha, R.J. (1973), *Generalized Simulation Technique for Turbojet Engine System Analysis*, NASA TN D-6610.

Sellers, J. and Daniele, C.J. (1974), *Dyngen: A Program for Calculating Steady-State and Transient Performance of Turbojet and Turbofan Engines*, NASA TM X-71552.

Wang, L. (2011), "A general multitask simulation package of aircraft engine", *Proc. Eng.*, **12**, 47-53.

Xu, L., Hynes, P.T. and Denton, J.D. (2003), "Towards long length scale unsteady modelling in turbomachines", IMechE Part A, *J. Pow. Energy*, **217**(1), 75-82.

Zheng, J., Chen, M. and Tang, H. (2017), "Matching mechanism analysis on an adaptive cycle engine", *Chin. J. Aeronaut.*, **30**(2), 706-718.

EC